PERGAMON

International Journal of Solids and Structures 37 (2000) 6011–6029

INTERNATIONAL JOURNAL OF SOLIDS and STRUCTURES

www.elsevier.com/locate/ijsolstr

Limit state analysis of reinforced concrete plates subjected to in-plane forces

Peter Noe Poulsen, Lars Damkilde*

Department of Structural Engineering and Materials, Technical University of Denmark, Building 118, 2800 Lyngby, Denmark

Received 3 March 1998; in revised form 7 September 1999

Abstract

A finite element formulation of rigid-plastic plates subjected to in-plane forces is developed using stress-based elements and linear programming. Three elements are established, namely a triangular plate element, a bar element and a beam element. The problem is formulated as a lower bound solution, and the dual variables are interpreted as displacements. Both load and material optimization are formulated. The method is applied to concrete plate structures modeling both the distributed and the concentrated reinforcement. An efficient computational scheme is used, thereby reducing the size of the problem. Finally, numerical examples are presented to show the capabilities of the method.

Keywords: Concrete; Finite element; Limit load analysis; Numerical methods; Optimization

1. Introduction

Calculation of the ultimate load carrying capacity for reinforced concrete structures such as slabs or plates is often based on the assumption of a perfect plastic material behavior. The calculation methods are either based on the lower bound theorem or the upper bound theorem. The upper bound method seeks a feasible collapse mode for which the load carrying capacity is minimal, whereas the lower bound method seeks a stress distribution in equilibrium for which the load carrying capacity is maximal.

Originally, calculations were made manually and the yield-line method, developed by Johansen (1972), was a pioneering work. The first numerical approaches to the perfect plasticity assumption date back to the 1970s where frame structures (Grierson and Gladwell, 1971) and slabs (Anderheggen and Knöpfel,

* Corresponding author. Fax: +45-45-88-32-82.
E-mail address: ld@bkm.dtu.dk (L. Damkilde).

0020-7683/00/$ - see front matter
PII: S0020-7683(99)00254-1

Nomenclature

A	area of element
A_x, A_y	area of reinforcement per length in x- and y-direction
a_i, b_i	coordinate difference in x- and y-direction for element side i
$\boldsymbol{C}$	constraint matrix
$\bar{\boldsymbol{C}}$	compact constraint matrix
$\boldsymbol{C}_\mathrm{d}$	material constraint matrix
$\boldsymbol{C}_\mathrm{s}$	strength vector
f_c	compressive strength of concrete
f_t^x, f_t^y	tensile strength in x- and y-direction
f_y	yield stress of reinforcement
$\boldsymbol{h}$	element equilibrium matrix
$\boldsymbol{H}$	system equilibrium matrix
l, l_i	length of element and element side i
M	moment
N	normal force
p_x, p_y	load intensity in the x- and y-direction
$\boldsymbol{q}$	element nodal force vector
$\boldsymbol{R}$	system load vector
t	thickness
$\boldsymbol{V}$	displacement vector
W	resistant moment
β	element stress parameter vector
β_s	system stress parameter vector
λ	scalar on variable load vector
ψ	plastic strain vector
σ_x, σ_y, τ	in-plane stresses

1972) were treated. Both upper and lower bound formulations were implemented in a finite element scheme well-known from linear elastic analysis.

Application of perfect plasticity to reinforced concrete plates is in large part due to Nielsen (1971, 1984), who has solved many practical problems. In recent years, this approach has received an increased interest due to a wider acceptance of perfect plasticity applications in the new Eurocode for concrete structures.

So far, numerical solutions to plate problems have seemed somewhat more complex than numerical solutions to slab problems. This is due to the fact that the elements have to be fairly complicated if the influence from concentrated reinforcement has to be taken into account. A simplified numerical solution based on the stringer method in which the plate is divided into rectangular shear elements with concentrated orthogonal reinforcement was formulated by Damkilde et al. (1994b). However, as this type of analysis has a rather limited scope, the aim of the present work is to cover a wider range of applications.

The calculation method is based on the lower bound method, and the stress field is described via a finite element discretization where the elements have stress parameters. As the structure is statically indeterminate only a part of the stress parameters are needed to secure equilibrium, whereas the rest can

be used to redistribute the load in order to maximize the load carrying capacity. The yield criteria are linearized and the formulation thereby becomes a Linear Programming (LP)-problem. In addition the collapse mode can be identified as the solution to the dual LP-problem, and the displacements can be identified as the marginal prices for the equilibrium equations. The method also enables optimization of the material for given loadcases. A triangular element with linear stress variation is established along with compatible bar and beam elements. Previously, a similar triangular element was used in soil mechanics (Sloan, 1988).

For the design of concrete plates there exists different methods, based on the assumption that the material behavior for both concrete and reinforcement can be regarded as plastic. The main differences lie in the determination of the deformations in the plate. Application of perfect plastic models implicitly assumes sufficient deformation capabilities in the structure in order to allow for the redistribution of forces. This approach is used in this context and has been applied by others, see e.g. Ashour and Morley (1994). One major advantage of the perfect plastic models is the possibility of direct optimization of e.g. the reinforcement.

A full non-linear analysis of the problem has been used by Blaauwendraad and Hoogenboom (1996, 1997). Physically, this approach is the most correct one. However, their finite element formulation is not established as an optimization method based on LP. Anderheggen et al. (1994) used a more ad hoc based solution principle. The idea was to generate different equilibrium systems by considering several systems of fictitious initial strains, superposed upon the elastic solution. This method does not give the load-displacement curve and, therefore, it cannot give information on the formation of cracks.

In concrete design the Strut-and-Tie models (Marti, 1985; Schlaich et al., 1987) have been received with great interest. The basic idea is to define a system of struts and ties which carries the loads in compression and tension as illustrated in Fig. 1(a). The method is based on an engineering judgement, and a number of guidelines have been established for choosing an optimal way of carrying the loads. The plastic redistribution of stresses is only taken into account indirectly by choosing *natural* ways of carrying the load. The Strut-and-Tie models have been applied by many authors to solve practical design problems (Schlaich and Schäfer, 1991; Zielinski and Rigotti, 1995; Yun and Ramirez, 1996). Typical problems concern reinforcement around holes, at supports or in corner regions. A weakness in the method is that the stress state is not necessarily optimal as it primarily consist of members in pure tension or compression. The only zones with a biaxial stress state is the small regions where the tension/compression members meet. This limitation exists e.g. in the modeling of a biaxial arch action, see Marti (1985). The Strut-and-Tie model can be considered as a lower bound method, and our numerical approach can be considered as an enhanced model. In Fig. 1(b) a finite element mesh of the same problem is illustrated. The advantages of our approach are that it is not necessary to make any assumptions to the stress pattern, and that the analysis determines the optimal stress distribution.

2. Formulation

In the limit state analysis the lower bound method is applied. A lower bound solution is a stress state where

- Equilibrium is satisfied
- Yield criteria are not violated

The problem is discretized by the traditional Finite Element concept with stress-based elements. In a Finite Element context the discretized equilibrium equations are given by

$$\boldsymbol{H}\beta = \boldsymbol{R}_{\mathrm{c}} + \lambda \boldsymbol{R} \tag{1}$$

where β are the stress parameters and $\boldsymbol{H}$ the equilibrium matrix. The load consists of a constant part $\boldsymbol{R}_c$ and a part $\boldsymbol{R}$ proportional to a scalar load parameter λ. The equilibrium matrix $\boldsymbol{H}$ is composed of contributions from the individual elements, and formulas for the local equilibrium matrices are given in a later section. It should be noted, that the number of stress parameters generally exceeds the number of equilibrium equations.

In general, the yield criteria are non-linear functions of the stress and strength parameters. However, a linearization of the yield criteria is employed in order to ensure an efficient optimization. In each element the yield criteria are checked in a number of points. The number of points depend on the stress variations in the elements. The yield criteria for all elements can be stated as

$$\boldsymbol{C}\beta \leq \boldsymbol{C}_s \tag{2}$$

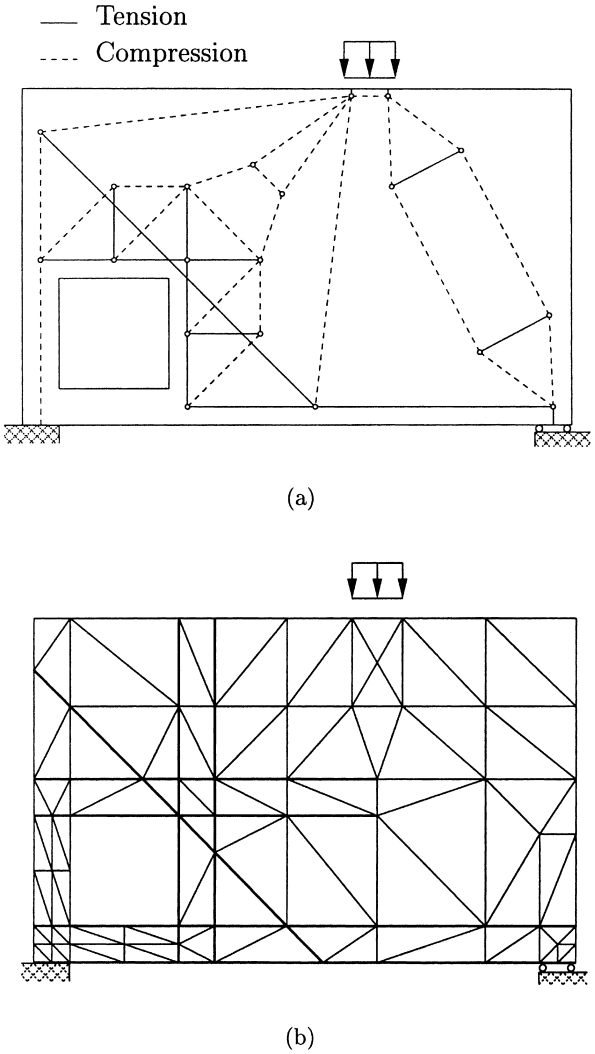

Fig. 1. (a) Strut-and-tie model; (b) finite element model.

where each row represents a linearized yield criterion. The values in $\boldsymbol{C}$ depend on the linearization planes, whereas the values in $\boldsymbol{C}_{\mathrm{s}}$ depend on the material strengths.

The objective is to determine the optimal stress distribution which maximizes the external load for a given structure or which minimizes the material costs for a given load. Due to the linearized yield criteria the optimization problem results in a LP-problem. The LP-problem for load optimization is given as

$$\text{maximize:} \quad \begin{Bmatrix} \mathbf{0}^{\mathrm{T}} & 1 \end{Bmatrix} \begin{Bmatrix} \beta \\ \lambda \end{Bmatrix}$$

$$\text{restrictions:} \quad \begin{bmatrix} \boldsymbol{H} & -\boldsymbol{R} \\ \boldsymbol{C} & \mathbf{0} \end{bmatrix} \begin{Bmatrix} \beta \\ \lambda \end{Bmatrix} = \begin{Bmatrix} \boldsymbol{R}_{\mathrm{c}} \\ \boldsymbol{C}_{\mathrm{s}} \end{Bmatrix} \tag{3}$$

The solution gives the optimal value of the object function λ and the corresponding stress parameters β. Furthermore the marginal or shadow prices of the restrictions are determined. The marginal price is defined as the increase in the object function for a unit change in the limiting value in the right-hand side. Thus a marginal price of 0 means that the restriction is not actually limiting the optimal value.

According to the general theory of LP (Luenberger, 1989), each primal LP-problem has a dual counterpart, which can be derived directly from the original problem. The dual LP-problem for the load optimization problem is given as

$$\text{minimize:} \quad \begin{Bmatrix} \boldsymbol{R}_{\mathrm{c}}^{\mathrm{T}} & \boldsymbol{C}_{\mathrm{s}}^{\mathrm{T}} \end{Bmatrix} \begin{Bmatrix} -\boldsymbol{V} \\ \psi \end{Bmatrix}$$

$$\text{restrictions:} \quad \begin{bmatrix} \boldsymbol{H}^{\mathrm{T}} & \boldsymbol{C}^{\mathrm{T}} \\ -\boldsymbol{R}^{\mathrm{T}} & \mathbf{0}^{\mathrm{T}} \end{bmatrix} \begin{Bmatrix} -\boldsymbol{V} \\ \psi \end{Bmatrix} = \begin{Bmatrix} 0 \\ 1 \end{Bmatrix} \tag{4}$$

where the dual variables $\boldsymbol{V}$ and ψ can be interpreted as the displacements and the plastic strains, respectively (Krenk et al., 1994). The optimal solution for the primal problem is also the optimal solution for the dual problem. The displacements correspond to the marginal-prices of the equilibrium equations, whereas the plastic strains correspond to the marginal prices of the yield criteria. For the discretized problem the optimal solution is both a lower and upper bound solution.

In material optimization design variables $\boldsymbol{d}$ are added. In order to maintain the linear programming problem the yield criteria must be linear in the design variables as shown

$$\boldsymbol{C}\beta + \boldsymbol{C}_{\mathbf{d}} d \leq \boldsymbol{C}_{\mathrm{s}} \tag{5}$$

where $\boldsymbol{C}_{\mathrm{d}}$ depends on the linearization of the yield criteria.

In material optimization the load is given, but several loadcases may exist. The stress parameters differ from loadcase to loadcase, and shakedown is not considered. For n loadcases the LP-problem is defined as

$$\text{minimize:} \quad \begin{Bmatrix} \mathbf{0}^{\mathrm{T}} & \cdots & \mathbf{0}^{\mathrm{T}} & \boldsymbol{a}^{\mathrm{T}} \end{Bmatrix} \begin{Bmatrix} \beta^1 \\ \vdots \\ \beta^n \\ \boldsymbol{d} \end{Bmatrix}$$

$$\text{restrictions:}\quad \begin{bmatrix} \boldsymbol{H} & & & \\ & \ddots & & \\ & & \boldsymbol{H} & \\ \boldsymbol{C} & & & \boldsymbol{C}_{\mathrm{d}} \\ & \ddots & & \vdots \\ & & \boldsymbol{C} & \boldsymbol{C}_{\mathrm{d}} \end{bmatrix} \begin{Bmatrix} \beta^1 \\ \vdots \\ \beta^n \\ d \end{Bmatrix} \begin{matrix} = \\ \vdots \\ = \\ \leq \\ \vdots \\ \leq \end{matrix} \begin{Bmatrix} \boldsymbol{R}^1 \\ \vdots \\ \boldsymbol{R}^n \\ \boldsymbol{C}_{\mathrm{s}} \\ \vdots \\ \boldsymbol{C}_{\mathrm{s}} \end{Bmatrix} \tag{6}$$

where the content of $\boldsymbol{a}$ are the material weights reflecting the cost of the corresponding design variables.

Practical design requirements, such as minimum and maximum of design variables, are not included in Eq. (6) but fit directly in the LP-problem.

The LP-problems for load and material optimization can be written in a compact form using only the statically indeterminated stress parameters and thereby reducing the number of variables (Damkilde and Høyer, 1993). The compact form of the LP-problems are given in Appendix A. The limit state analysis of plates has been implemented in the system limitS (Damkilde and Krenk, 1997) which also covers limit state analysis of slabs and frames.

3. Finite element formulation

In order to be able to model plates with arbitrary geometry and concentrated reinforcement three different elements are needed, namely a triangular plate element, a bar element and a beam element. The bar and beam elements are compatible with the plate element and can be used along the sides of the plate element.

The equilibrium equations for an element can be given in a compact notation

$$\boldsymbol{q} = \boldsymbol{h}\beta \tag{7}$$

where $\boldsymbol{h}$ is the equilibrium matrix and the content of $\boldsymbol{q}$ are the generalized external nodal forces in equilibrium with the stress parameters β. The contributions from the element equilibrium matrices $\boldsymbol{h}$ are assembled in the equilibrium matrix $\boldsymbol{H}$ for the total system similarly to the Finite Element method. The generalized nodal forces can be either stresses, forces or moments depending on the type of the equations. Some of the equilibrium equations secure continuity in the stresses across element sides whereas other secure equilibrium between forces or moments from intersecting line elements. The practical organization is a topological problem well-known from standard Finite Element techniques.

3.1. Plate element

The stress variation in the triangular plate element is chosen to be linear and the stresses within the element are, therefore, interpolated linearly from values at the corner nodes. The element is similar to an element previously formulated by Sloan (1988). With the three stresses σ_x, σ_y and τ at each node the number of stress parameters per element are nine.

The equilibrium matrix for a plate element can be written as

$$\begin{Bmatrix} \boldsymbol{q}_1 \\ \boldsymbol{q}_2 \\ \boldsymbol{q}_3 \\ \boldsymbol{q}_{\mathrm{c}} \end{Bmatrix} = \begin{bmatrix} \boldsymbol{h}_1 & & \\ & \boldsymbol{h}_2 & \\ & & \boldsymbol{h}_3 \\ \boldsymbol{h}_{\mathrm{c}1} & \boldsymbol{h}_{\mathrm{c}2} & \boldsymbol{h}_{\mathrm{c}3} \end{bmatrix} \begin{Bmatrix} \beta_1 \\ \beta_2 \\ \beta_3 \end{Bmatrix} \tag{8}$$

where the numbers 1, 2 and 3 refers to the nodes shown in Fig. 2 and the letter c refers to the center of the element.

The nine stress parameters in the element have to fulfil the local equilibrium leading to two interior equilibrium equations formulated in the x- and y-directions

$$\sigma_{x,\,x} + \tau_{,y} + p_x = 0$$

$$\sigma_{y,\,y} + \tau_{,x} + p_y = 0 \tag{9}$$

where p_x and p_y are the distributed loads per unit area in the x- and y-directions, respectively. As the stresses are chosen to vary linearly p_x and p_y have to be constant over the element. The equilibrium equations consist of two parts namely the external load and the contributions from the stress parameters which can be written as generalized nodal forces, see Eq. (7). The equilibrium is secured by the balance of these two parts. The external load enters the right-hand side in Eq. (1). The generalized nodal forces corresponding to the distributed load are referred to the central node, see Fig. 2. The part of Eq. (9) corresponding to the stress parameters is established as a sum of the contributions from each corner node

$$\boldsymbol{q}_{\mathrm{c}} = \begin{Bmatrix} q_x \\ q_y \end{Bmatrix} = \boldsymbol{q}_{\mathrm{c}1} + \boldsymbol{q}_{\mathrm{c}2} + \boldsymbol{q}_{\mathrm{c}3} \tag{10}$$

where the contribution from the stresses at node i can be written as

$$\boldsymbol{q}_{\mathrm{c}i} = \begin{bmatrix} \dfrac{b_i}{2A} & 0 & -\dfrac{a_i}{2A} \\ 0 & -\dfrac{a_i}{2A} & \dfrac{b_i}{2A} \end{bmatrix} \begin{Bmatrix} t\sigma_x^i \\ t\sigma_y^i \\ t\tau^i \end{Bmatrix} = \boldsymbol{h}_{\mathrm{c}i}\beta_i \tag{11}$$

where $\boldsymbol{h}_{\mathrm{c}i}$ depend on the geometry of the element. The area of the element is A and the geometry of the triangle is defined by the coordinates of the three corner nodes (x_i, y_i) where i takes the value 1, 2 and 3. Side i opposite node i is considered as a vector (a_i, b_i), with the length l_i

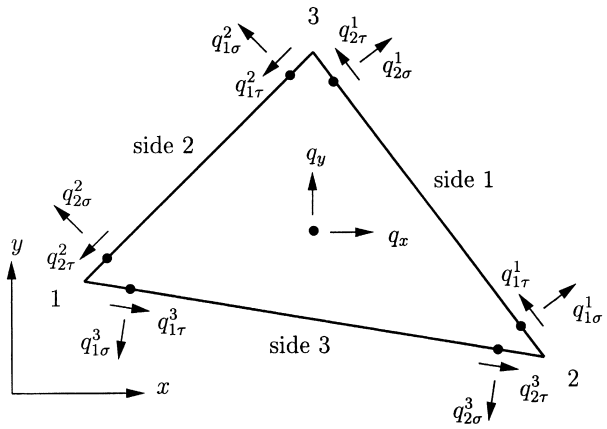

Fig. 2. Generalized nodal forces.

$$a_i = x_k - x_j \quad b_i = y_k - y_j \quad l_i = \sqrt{a_i^2 + b_i^2} \tag{12}$$

where i, j and k are a permutation of 1, 2 and 3.

Furthermore, the system must ensure equilibrium of stresses across element boundaries. For the plate element this applies to the stresses normal to the sides as well as to the shear stresses, while the stresses parallel to the sides can be discontinuous. As the stress variation is linear the equilibrium equations is established in two points along a side. For convenience these equations are established at the ends of each side, see Fig. 2. The generalized nodal forces at node i are given solely by the internal stresses at node i, see Eq. (8). The terms in the equilibrium matrix stemming from the stresses at node i are given as

$$\boldsymbol{q}_i = \begin{Bmatrix} q^j_{2\sigma} \\ q^j_{2\tau} \\ q^k_{1\sigma} \\ q^k_{1\tau} \end{Bmatrix} = \begin{bmatrix} \frac{b_j^2}{l_j^2} & \frac{a_j^2}{l_j^2} & -\frac{2a_jb_j}{l_j^2} \\ \frac{a_jb_j}{l_j^2} & -\frac{a_jb_j}{l_j^2} & \frac{b_j^2 - a_j^2}{l_j^2} \\ \frac{b_k^2}{l_k^2} & \frac{a_k^2}{l_k^2} & -\frac{2a_kb_k}{l_k^2} \\ \frac{a_kb_k}{l_k^2} & -\frac{a_kb_k}{l_k^2} & \frac{b_k^2 - a_k^2}{l_k^2} \end{bmatrix} \begin{Bmatrix} t\sigma^i_x \\ t\sigma^i_y \\ t\tau^i \end{Bmatrix} = \boldsymbol{h}_i\beta_i \tag{13}$$

By use of Eqs. (8), (11) and (13) the equilibrium matrix for the plate element can be established.

If an element has two sides on an inner or outer boundary the stress continuity demands in Eq. (13) result in four constraints on the three internal stress parameters at the corner node which connects these two sides. The redundant constraint can be eliminated geometrically or a non full rank may be accepted in the factorization of the equilibrium equations (1).

3.2. Bar and beam elements

A bar element with axial force and a beam element with bending moments are established. The bar and beam elements are used for modeling concentrated reinforcement and steel members, respectively. The beam element is also necessary in order to model curved reinforcement with straight elements as the bar element cannot transfer the axial force from one element to another. The beam element reflects the physical action and introduces compressive stresses, perpendicular to the beam element, in the neighbouring plate elements.

To ensure proper interaction with plate elements the stress variation of the bar element must correspond to a linear varying axial load. This leads to a quadratic variation of the normal force, and three stress parameters are, therefore needed, see Fig. 3 where the generalized nodal forces are also shown.

The equilibrium matrix for the bar element is given as

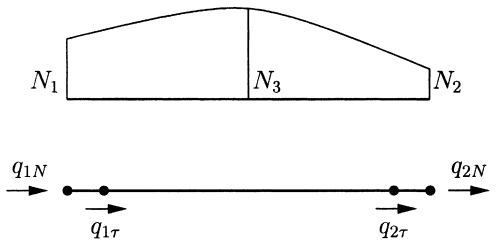

Fig. 3. Stress parameters and generalized nodal forces for a bar element.

$$\begin{Bmatrix} q_{1N} \\ q_{1\tau} \\ q_{2N} \\ q_{2\tau} \end{Bmatrix} = \begin{bmatrix} -1 & 0 & 0 \\ \frac{3}{l} & \frac{1}{l} & -\frac{4}{l} \\ 0 & 1 & 0 \\ -\frac{1}{l} & -\frac{3}{l} & \frac{4}{l} \end{bmatrix} \begin{Bmatrix} N_1 \\ N_2 \\ N_3 \end{Bmatrix} \tag{14}$$

where the generalized nodal forces $q_{1\tau}$ and $q_{2\tau}$ are shear stresses times the plate thickness, which act together with the appropriate shear contributions from Eq. (13) to ensure equilibrium along the bar element. The generalized nodal forces q_{1N} and q_{2N} are normal forces which may act together with forces from adjacent bar or beam elements.

In order to ensure proper equilibrium interaction with plate elements the stress variation of the beam element must correspond to a linear transverse load. This leads to a cubic stress variation with four stress parameters, see Fig. 4 where the generalized nodal forces are also shown.

The equilibrium matrix for the beam element is given as

$$\begin{Bmatrix} q_{1V} \\ q_{1M} \\ q_{1\sigma} \\ q_{2V} \\ q_{2M} \\ q_{2\sigma} \end{Bmatrix} = \begin{bmatrix} -\frac{11}{2l} & \frac{2}{2l} & \frac{18}{2l} & -\frac{9}{2l} \\ -1 & 0 & 0 & 0 \\ -\frac{18}{l^2} & \frac{9}{l^2} & \frac{45}{l^2} & -\frac{36}{l^2} \\ \frac{2}{2l} & -\frac{11}{2l} & -\frac{9}{2l} & \frac{18}{2l} \\ 0 & 1 & 0 & 0 \\ \frac{9}{l^2} & -\frac{18}{l^2} & -\frac{36}{l^2} & \frac{45}{l^2} \end{bmatrix} \begin{Bmatrix} M_1 \\ M_2 \\ M_3 \\ M_4 \end{Bmatrix} \tag{15}$$

where the generalized nodal forces $q_{1\sigma}$ and $q_{2\sigma}$ are normal stresses times the plate thickness. Similarly to the bar element these stresses act together with the appropriate contributions from the plate element Eq. (13) to ensure equilibrium along the beam element. The generalized nodal forces q_{1V} and q_{2V} are shear forces which may act together with forces from adjacent bar or beam elements. The generalized nodal forces q_{1M} and q_{2M} are moments and they act together with moments from adjacent beam elements.

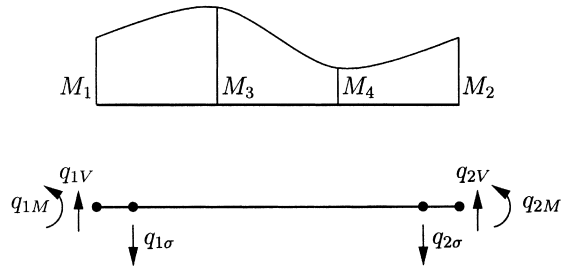

Fig. 4. Stress parameters and generalized nodal forces for a beam element.

3.3. Displacements for dual problem

The dual interpretation of the linear programming problem enables the determination of the collapse form of the structure. The marginal price of the end nodes in the bar and the beam elements can be directly interpreted as the displacement in the node. The midside nodes which state equilibrium along the element side, require a scaling of the marginal price. A distributed load with the intensity 1 at one end gives a total load $l/2$, where l is the length of the side. Thus, the displacements have to be scaled with the factor $2/l$ and be referred to the centre of gravity at one third of the length. The same applies to the plate element, i.e. the equilibrium equations at the center are to be scaled by $1/A$, where A is the area of the element. The displacements of the plate element reproduce the rigid part of the collapse mode, but the additional part is not physically illustrative.

4. Yield criteria

In order to formulate a linear programming problem the yield criteria must be linear in the stress variables. The yield criteria for a reinforced plate and for a beam are non-linear and subsequently have to be linearized.

4.1. Plate

Nielsen (1984) proposed the yield criterion shown in Fig. 5 for a reinforced plate. The yield criterion is given by the equations

$$-\left(f_{\mathrm{t}}^{x}-\sigma_x\right)\left(f_{\mathrm{t}}^{y}-\sigma_y\right)+\tau^2=0$$

$$-(f_{\mathrm{c}}+\sigma_x)\left(f_{\mathrm{c}}+\sigma_y\right)+\tau^2=0 \tag{16}$$

where f_{c} is the compressive strength and the tensile strengths are

$$f_{\mathrm{t}}^{x}=\frac{A_x f_{\mathrm{Y}}^{x}}{t}$$

$$f_{\mathrm{t}}^{y}=\frac{A_y f_{\mathrm{Y}}^{y}}{t} \tag{17}$$

where t is the thickness, A_x and A_y are areas of reinforcement per length and f_{Y}^x and f_{Y}^y are the yield stresses of the reinforcement in the x- and y-directions, respectively. The yield criterion is shown in Fig. 5.

In the case of load optimization, i.e. where the material parameters of the plate are known, the size of the yield surface is fixed beforehand. This makes it possible to linearize from the top of the cones to points on the elliptic intersection of the cones as indicated by the straight lines in Fig. 5. The ellipse is transformed into a circle which can be approximated as desired. The transformation from points on the circle $s^2 + t^2 = 1$ to the actual stresses is given as

$$\sigma_x = \frac{1}{2}\left(f_{\mathrm{t}}^x - f_{\mathrm{c}}\right) + \frac{1}{2}s\left(f_{\mathrm{t}}^x + f_{\mathrm{c}}\right)$$

$$\sigma_y = \frac{1}{2}\left(f_{\mathrm{t}}^y - f_{\mathrm{c}}\right) - \frac{1}{2}s\left(f_{\mathrm{t}}^y + f_{\mathrm{c}}\right)$$

$$\tau = \frac{1}{2}t\sqrt{\left(f_{\mathrm{t}}^x + f_{\mathrm{c}}\right)\left(f_{\mathrm{t}}^y + f_{\mathrm{c}}\right)} \tag{18}$$

In the case of material optimization the size and position of the yield surface is a function of the material parameters. Due to the non-linear expression in Eq. (16) it is impossible to use the same principle as in the case of load optimization. This would lead to non-linear expressions in the material parameters. Thus, in the case of material optimization the four lines in the base of the σ_x–σ_y-plane are used. These lines are linear in the material parameters. As the x–y directions have to be weighted equally, the slope of the planes has to be the same in both directions. The planes are now established using the maximum slope not violating the yield surface at any point, see Fig. 6.

$$\sigma_x + \tau < f_{\mathrm{t}}^x$$

$$-\sigma_x + \tau < f_{\mathrm{c}} \tag{19}$$

Similar restrictions apply to the y-direction and by changing the sign of the shear stresses it gives eight restrictions.

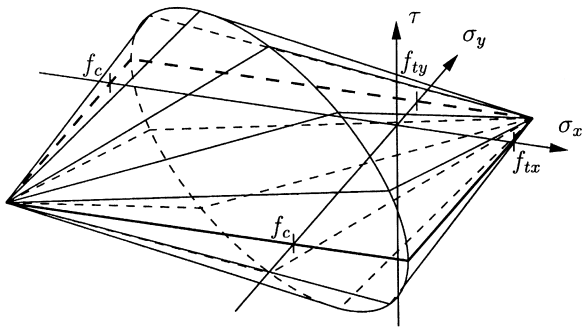

Fig. 5. Yield criteria for a plate.

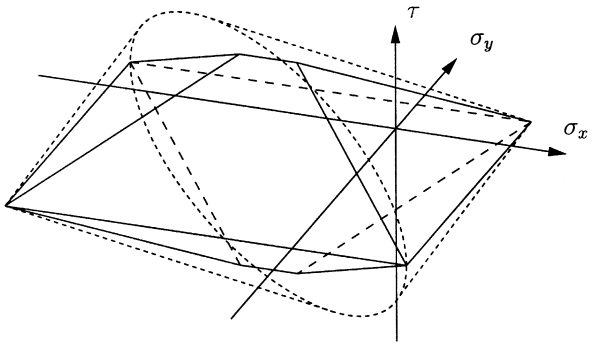

Fig. 6. Linearization of the yield surface in the case of material optimization.

4.2. Bar and beam

Linear yield criteria for a bar and a beam, respectively are given as

$$-Af_y \le N \le Af_y$$

$$-Wf_y \le M \le Wf_y \tag{20}$$

where f_y is the yield stress of the reinforcement, A is the area of reinforcement and Wf_y is the plastic moment capacity.

In a beam element with both normal and bending forces a combination of N and M is necessary. In the case of load optimization where the strengths are known a linearization, as shown in Fig. 7(a), is used. Whereas, in the case of material optimization the linearization in Fig. 7(b) is used in order for the restrictions to be linear in the material parameters.

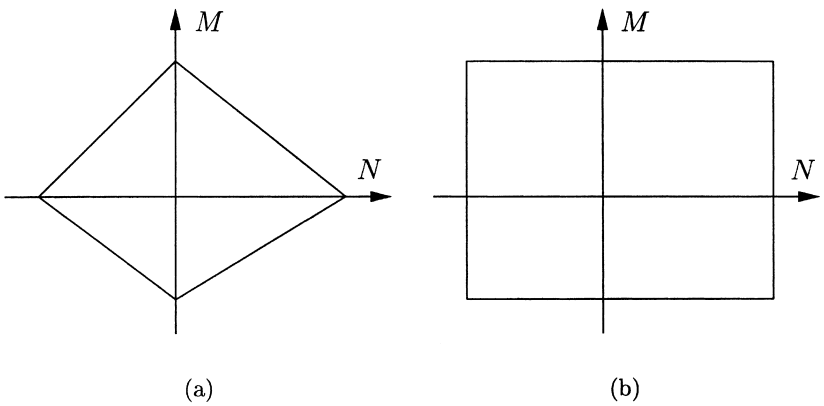

Fig. 7. Linearization of the yield surface for (a) load optimization; (b) material optimization.

5. Examples

5.1. Deep beam

The first example is a plate with isotropic reinforcement subjected to a uniform load at the top face, see Fig. 8(a). The example has an exact solution, see Nielsen (1984). This example is analysed with two different meshes, both shown in Fig. 8(a). The mesh shown on the left side in Fig. 8(a) corresponds to the exact solution which can be found by dividing the beam into four regions with constant stress. The element, which is capable of a linear stress variation, can therefore, reproduce the exact solution.

With the material parameters given in Fig. 8(b) the ultimate load capacity for the uniform mesh, shown on the right side in Fig. 8(a), is found to be 78% of the exact solution. In the exact solution the normal stress distribution in the middle section is compression in the upper part and tension in the lower part. The choice of the material parameters in Fig. 8(b) places the stress discontinuity in the upper element in the uniform mesh. This explains the relatively large difference in the ultimate load capacity. A refinement of the element mesh in the upper part would improve the result significantly.

5.2. End wall

The next example is a wall subjected to wind load which has previously been examined by Damkilde et al. (1994b) using the stringer method. The geometry, boundary conditions and wind load from the left are shown in Fig. 9(a). The element mesh is also shown in Fig. 9(a) where the bar elements are indicated by thick lines. The shear panels in the stringer method are divided into four elements in order to eliminate the dependency of the direction of the diagonals. The material parameters used in this example are where all plate elements have the same reinforcement. The same applies to bar elements. The ultimate load capacity, using 16 restrictions per yield surface, is found to be $\lambda = 106.84$ with wind from left and $\lambda = 104.29$ with wind from right. The stringer method gives the values $\lambda = 72.25$ and 74.34 which are approximately 30% lower than the values for the present method. This seems reasonably since

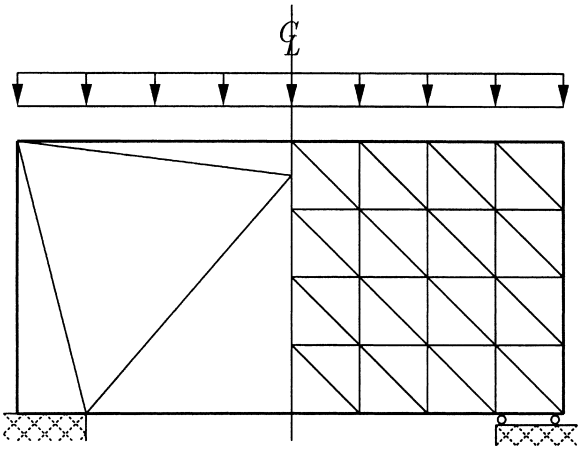

(a) Element meshes

$A_x = A_y = 500\,\mathrm{mm}^2/\mathrm{m}$

$t = 200\,\mathrm{mm}$

$f_Y^x = f_Y^y = 300\,\mathrm{MPa}$

$f_c = 20\,\mathrm{MPa}$

(b) Material parameters

Fig. 8. Deep beam example.

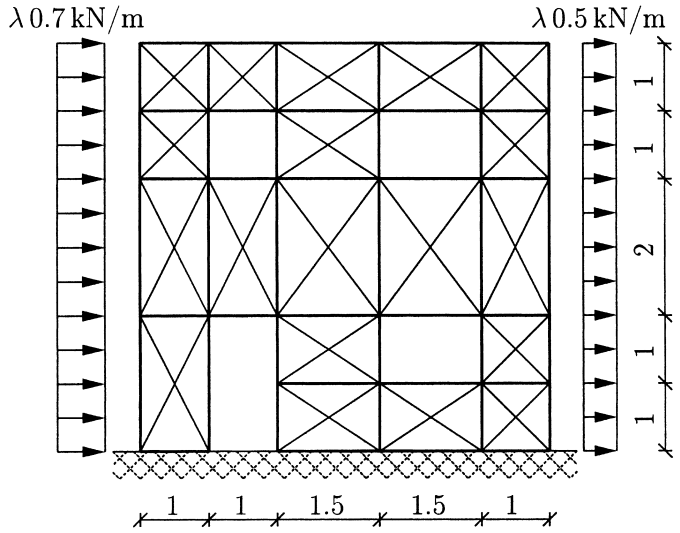

(a) Geometry, load and element mesh

$A = 500\,\mathrm{mm}^2$

$A_x = A_y = 400\,\mathrm{mm}^2/\mathrm{m}$

$t = 200\,\mathrm{mm}$

$f_Y^x = f_Y^y = 300\,\mathrm{MPa}$

$f_c = 15\,\mathrm{MPa}$

(b) Material parameters

Fig. 9. End wall.

the stringer method simplifies the stress distribution to tension–compression in the stringers and to pure shear in the shear panels. The plate element is capable of a more refined stress distribution combining normal stresses and shear stresses. The collapse mode is found by use of Eq. (26), and for the bar elements it is shown in Fig. 10.

For both loadcases, the collapse is seen to be a shear mode at the two bottom holes. In order to reduce the amount of reinforcement we consider material optimization with two loadcases, i.e with wind

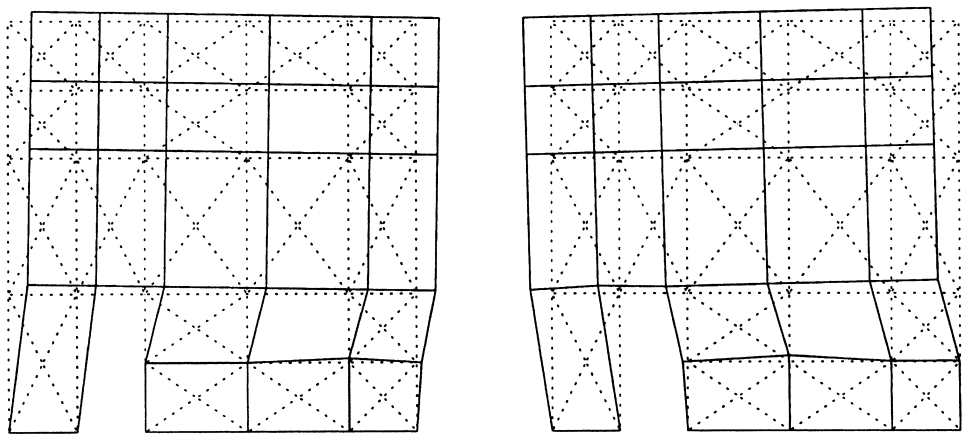

(a) (b)

Fig. 10. Collapse mode with wind from (a) left; (b) right.

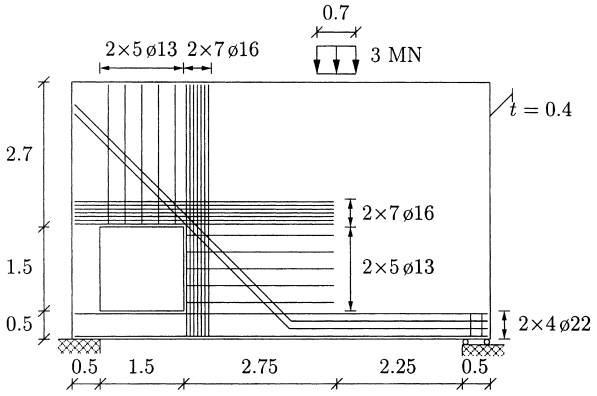

Fig. 11. Example with reinforcement design by Schlaich et al.

from both sides with $\lambda = 72.25$. The concentrated reinforcement in the bar elements has been chosen to be continuous in both directions except for the door hole. This gives six material parameters in each direction. Similarly, the distributed reinforcement has been chosen to be continuous except for holes. This gives four material parameters in the horizontal direction and five in the vertical direction. The amount of reinforcement is hereby reduced to 27.1×10^{-3} m^3 or 45.9% compared to the uniform reinforcement given in Fig. 9(b). For the stringer method these values are 37.0×10^{-3} m^3 and 62.6%.

5.3. Deep beam with hole

The last example is a deep beam with a large hole which has previously been analysed by Schlaich et al. (1987) using the Strut-and-Tie Model. The example and the main reinforcement arrangement, as designed by Schlaich et al., are shown in Fig. 11. Schlaich et al., suggest additional reinforcement such as a mesh on either surface of the wall, nominal column reinforcement at the left of the hole and stirrups below the hole. This example has also been analyzed by Blaauwendraad and Hoogenboom

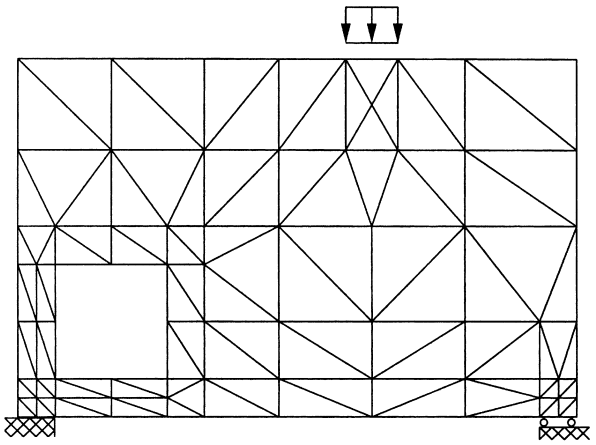

Fig. 12. Element model.

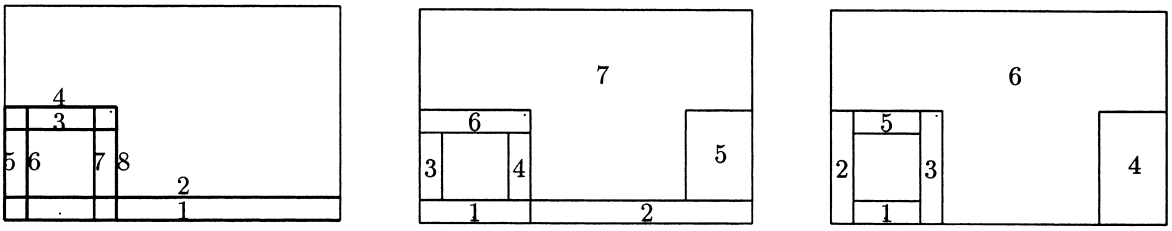

(a) Material parameters for concentrated reinforcement

(b) Material parameters for distributed reinforcement in the x-direction

(c) Material parameters for distributed reinforcement in the y-direction

Fig. 13. Material parameters.

(1996) using a stringer panel method. In their analysis a coarse model is used where the lower left corner, including the hole is left out. A model of this example, using the plate, bar and beam elements, is shown in Fig. 1(b). The thick lines in Fig. 1(b) indicate the bar and beam elements. Beam elements are used to model the bending of the diagonal reinforcement. The reinforcement arrangement by Schlaich et al. is used both as concentrated and as distributed reinforcement. Additional distributed reinforcement is added in both directions in order to carry the load 3 MN. This example is also analysed using material optimization. The chosen element model is shown in Fig. 12. There is a total of 21 material parameters, namely eight for the concentrated reinforcement and seven and six for the distributed reinforcement in the x- and y-direction, respectively, see Fig. 13. By using these material parameters the amount of reinforcement is reduced by 16%. Increasing the number of material parameters would presumably reduce the amount of reinforcement even more. However, for practical design reasons the number of material parameters should be limited.

6. Conclusion

Three stress-based elements are explicitly formulated in a general finite element concept. A method of calculating the load carrying capacity of a reinforced plate with concentrated reinforcement and beams is established. Furthermore, material optimization is established and provides an effective tool in determining the optimal reinforcement design of complex plate structures. The established plate element provides a more realistic stress distribution than, e.g. the stringer method or the Strut-and-Tie model which both simplifies the stress distribution. Due to the triangular form of the plate element any irregular geometries can be modelled. The above examples prove the effectiveness of the method.

Acknowledgements

Comments from an anonymous reviewer to a preliminary version of the paper are greatly appreciated.

Appendix A. Efficient computational implementation

The equilibrium equations (1) can be split up in to two parts $\boldsymbol{H}_0$ and $\boldsymbol{H}_1$, thereby identifying the

statically determinated stress parameters β_0. The number of statically determinated stress parameters equals the number of independent equilibrium equations. The matrix $\boldsymbol{H}_0$ has full rank and can be regarded as a statically determinated part of the structure carrying the external load in itself but with no possibility of redistributing stresses.

$$\begin{bmatrix} \boldsymbol{H}_0 & \boldsymbol{H}_1 \end{bmatrix} \begin{Bmatrix} \beta_0 \\ \beta_1 \end{Bmatrix} = \boldsymbol{R}_c + \lambda \boldsymbol{R} \tag{21}$$

The inverse matrix $\boldsymbol{H}_0^{-1}$ exists if the structure is sufficiently supported, and β_0 can be determined.

$$\beta_0 = \boldsymbol{H}_0^{-1}\left(\boldsymbol{R}_c + \lambda \boldsymbol{R} - \boldsymbol{H}_1 \beta_1\right) \tag{22}$$

For the plate problems the inverse matrix $\boldsymbol{H}_0^{-1}$ should be established using full pivoting in order to secure the most stable reduced linear programming problem. For frame and slab problems a partial pivoting scheme is sufficient.

With $\boldsymbol{C}$ partitioned as $\boldsymbol{H}$ in Eq. (21) the LP-problem for load optimization (3) can be written as a compact LP-problem

$$\text{maximize:} \quad \begin{Bmatrix} 0^T & 1 \end{Bmatrix} \begin{Bmatrix} \beta_1 \\ \lambda \end{Bmatrix}$$

$$\text{restrictions:} \quad \begin{bmatrix} \bar{\boldsymbol{C}} & \bar{\boldsymbol{C}}_\lambda \end{bmatrix} \begin{Bmatrix} \beta_1 \\ \lambda \end{Bmatrix} \leq \bar{\boldsymbol{C}}_s \tag{23}$$

where

$$\bar{\boldsymbol{C}} = \boldsymbol{C}_1 - \boldsymbol{C}_0 \boldsymbol{H}_0^{-1} \boldsymbol{H}_1$$

$$\bar{\boldsymbol{C}}_\lambda = \boldsymbol{C}_0 \boldsymbol{H}_0^{-1} \boldsymbol{R}$$

$$\bar{\boldsymbol{C}}_s = \boldsymbol{C}_s - \boldsymbol{C}_0 \boldsymbol{H}_0^{-1} \boldsymbol{R}_c \tag{24}$$

The advantage of this formulation is the reduced number of variables and restrictions. The LP-problem is solved using a LP-solver by Damkilde et al. (1994a). The LP-solver uses infinite variables and thereby reduces the problem compared to the traditional approach splitting each variable into two.

The dual problem to the compact LP-problem is

$$\text{minimize:} \quad \bar{\boldsymbol{C}}_s^T \psi$$

$$\text{restrictions:} \quad \begin{bmatrix} \bar{\boldsymbol{C}}^T \\ \bar{\boldsymbol{C}}_\lambda^T \end{bmatrix} \psi \begin{matrix} \leq \\ \leq \end{matrix} \begin{Bmatrix} 0 \\ 1 \end{Bmatrix} \tag{25}$$

This compact dual LP-problem for load optimization could also be found directly from Eq. (4) by using the same decomposition of $\boldsymbol{H}$ as in Eq. (21). This would give the relation

$$\boldsymbol{V} = \boldsymbol{H}_0^{T^{-1}} \boldsymbol{C}_0^T \psi \tag{26}$$

With a standard factorization of $\boldsymbol{H}$ in the form $\boldsymbol{L}\,\boldsymbol{D}\,\boldsymbol{U}$, where $\boldsymbol{L}$ and $\boldsymbol{U}$ are the lower and upper

triangular matrices, respectively and $\boldsymbol{D}$ the diagonal matrix, the inverse of $\boldsymbol{H}^{\mathrm{T}}$ can be found by backsubstitution using $\boldsymbol{U}^{\mathrm{T}}\boldsymbol{D}\boldsymbol{L}^{\mathrm{T}}$ and thereby avoiding extra factorization.

By use of the dual variables from the LP-problem (3) the collapse mode can be found from Eq. (26).

The compact LP-problem in the case of material optimization is found by use of the same decomposition of $\boldsymbol{H}$ as in Eq. (21). This gives

$$\text{minimize:} \quad \left\{ 0^{\mathrm{T}} \quad \cdots \quad 0^{\mathrm{T}} \quad \boldsymbol{a}^{\mathrm{T}} \right\} \begin{Bmatrix} \beta_1^1 \\ \vdots \\ \beta_1^n \\ \boldsymbol{d} \end{Bmatrix}$$

$$\text{restrictions:} \quad \begin{bmatrix} \bar{\boldsymbol{C}} & & \boldsymbol{C}_{\mathbf{d}} \\ & \ddots & \vdots \\ & & \bar{\boldsymbol{C}} \quad \boldsymbol{C}_{\mathrm{d}} \end{bmatrix} \begin{Bmatrix} \beta_1^1 \\ \vdots \\ \beta_1^n \\ d \end{Bmatrix} \begin{matrix} \leq \\ \vdots \\ \leq \end{matrix} \begin{Bmatrix} \bar{\boldsymbol{C}}_{\mathrm{s}}^1 \\ \vdots \\ \bar{\boldsymbol{C}}_{\mathrm{s}}^n \end{Bmatrix} \tag{27}$$

where $\bar{\boldsymbol{C}}$ is given in Eq. (24) and

$$\bar{\boldsymbol{C}}_{\mathrm{s}}^i = \boldsymbol{C}_{\mathrm{s}} - \boldsymbol{C}_0 \boldsymbol{H}_0^{-1} \boldsymbol{R}^i \tag{28}$$

The compact dual LP-problem for material optimization is

$$\text{maximize:} \quad \left\{ \bar{\boldsymbol{C}}_{\mathrm{s}}^{1^{\mathrm{T}}} \quad \cdots \quad \bar{\boldsymbol{C}}_{\mathrm{s}}^{n^{\mathrm{T}}} \right\} \begin{Bmatrix} \psi^1 \\ \vdots \\ \psi^n \end{Bmatrix}$$

$$\text{restrictions:} \quad \begin{bmatrix} \bar{\boldsymbol{C}}^{\mathrm{T}} & & \\ & \ddots & \\ & & \bar{\boldsymbol{C}}^{\mathrm{T}} \\ \boldsymbol{C}_{\mathrm{d}}^{\mathrm{T}} & \cdots & \boldsymbol{C}_{\mathrm{d}}^{\mathrm{T}} \end{bmatrix} \begin{Bmatrix} \psi^1 \\ \vdots \\ \psi^n \end{Bmatrix} \begin{matrix} = \\ \vdots \\ = \\ \leq \end{matrix} \begin{Bmatrix} \mathbf{0} \\ \vdots \\ \mathbf{0} \\ \boldsymbol{a} \end{Bmatrix} \tag{29}$$

where the displacements can be found from

$$\boldsymbol{V}^i = \boldsymbol{H}_0^{\mathrm{T}^{-1}} \boldsymbol{C}_0^{\mathrm{T}} \psi^i \tag{30}$$

References

Anderheggen, E., Knöpfel, H., 1972. Finite element limit analysis using linear programming. International Journal of Solids and Structures 8, 1413–1431.

Anderheggen, E., Despot, Z., Steffen, P., Tabatabai, S.M.R., 1994. Reinforced-concrete dimensioning based on element nodal forces. Journal of Structural Engineering 120 (6), 1718–1731.

Ashour, A.F., Morley, C.T., 1994. The numerical determination of shear failure mechanisms in reinforced-concrete beams. The Structural Engineer 72 (23, 24), 395–400.

Blaauwendraad, J., Hoogenboom, P.C.J., 1996. Stringer panel model for structural concrete design. ACI Structural Journal 93 (3), 295–305.

Blaauwendraad, J., Hoogenboom, P.C.J., 1997. Discrete elements in structural concrete design. HERON 42 (3), 159–168.

Damkilde, L., Høyer, O., 1993. An efficient implementation of limit state calculations based on lower-bound solutions. Computers and Structures 49 (6), 953–962.

Damkilde, L., Krenk, S., 1997. Limits — a system for limit state analysis and optimal material layout. Computers and Structures 64 (1-4), 709–718.

Damkilde, L., Høyer, O., Krenk, S., 1994a. A direct linear programming solver in c for structural applications. Computers and Structures 52 (3), 511–528.

Damkilde, L., Olsen, J.F., Poulsen, P.N., 1994b. A program for limit state analysis of plane, reinforced concrete plates by the stringer method. Bygningsstatiske Meddelelser 65 (1), 1–26.

Grierson, D.E., Gladwell, G.M.L., 1971. Collapse load analysis using linear programming. Journal of the Structural Engineering Division, ASCE 97 (5), 1561–1573.

Johansen, K.W., 1972. Yield-Line Formulae for Slabs. Cement and Concrete Association, London, UK.

Krenk, S., Damkilde, L., Høyer, O., 1994. Limit analysis and optimal design of plates with equilibrium elements. Journal of Engineering Mechanics 120 (6), 1237–1254.

Luenberger, D.G., 1989. Linear and Nonlinear Programming. Addison-Wesley, Reading, MA.

Marti, P., 1985. Basic tools of reinforced concrete beam design. ACI Structural Journal 82 (4), 46–56.

Nielsen, M.P., 1971. On the Strength of Reinforced Concrete Discs. Acta Polytechnia Scandinavica.

Nielsen, M.P., 1984. Limit Analysis and Concrete Plasticity. Prentice-Hall, Englewood Cliffs, NJ.

Schlaich, J., Schäfer, K., 1991. Design and detailing of structural concrete using strut-and-tie models. The Structural Engineer 69 (6), 113–125.

Schlaich, J., Schäfer, K., Jennewein, M., 1987. Toward a consistent design of structural concrete. PCI Journal, Special Report, Vol. 32, 74–150.

Sloan, S.W., 1988. Lower bound limit analysis using finite elements and linear programming. International Journal for Numerical and Analytical Methods in Geomechanics 12, 61–77.

Yun, Y.M., Ramirez, J.A., 1996. Strength of struts and nodes in strut-tie model. Journal of Structural Engineering 122 (1), 20–29.

Zielinski, Z.A., Rigotti, M., 1995. Tests on shear capacity of reinforced concrete. Journal of Structural Engineering 121 (11), 1660–1666.